Journal of Biomechanics 180 (2025) 112517

Contents lists available at ScienceDirect

Journal of Biomechanics

journal homepage: www.elsevier.com/locate/jbiomech

The influence of simulated worn shoe and foot inversion on heel internal biomechanics during running impact: A subject-specific finite element analysis

Yang Song [a], Xuanzhen Cen [b], Meizi Wang [a], Kovács Bálint [b,c], Qitao Tan [a], Dong Sun [b], Shunxiang Gao [b], Fengping Li [b], Yaodong Gu [b], Yan Wang [a,*], Ming Zhang [a]

[a] Department of Biomedical Engineering, The Hong Kong Polytechnic University, Hong Kong Special Administrative Region
[b] Faculty of Sports Science, Ningbo University, Ningbo, China
[c] Department of Kinesiology, Hungarian University of Sports Science, Budapest, Hungary

ARTICLE INFO

Keywords:
Running
Worn footwear
Foot inversion
Foot biomechanics
Finite element analysis

ABSTRACT

This study explored how systematic changes in running shoe degradation and foot inversion alter the distribution and peak value of heel pressure and calcaneus stress, as well as the total stress-concentration exposure (TSCE) within the calcaneal bone. A foot-shoe finite element model was employed and three shoe wear conditions (new shoe (CON), moderate worn shoe (MWSC), excessive worn shoe (EWSC)) coupled with three foot inversion angles (0°, 10°, 20°) were further modulated. Simulations were conducted at the impact peak instant during running. Compared to CON0, heel pressure during neutral landings shifted medially and increased with progressive shoe wear, peaking under EWSC0. This shift expanded the high-pressure area by 1.333 cm^2 and raised peak pressure by 24.42 %. Foot inversion landings exhibited an opposite trend: increased shoe wear promoted balanced pressure distribution, centralizing the load and eliminating high-pressure areas under EWSC10, where peak pressure was 11.36 % lower than CON10. Calcaneus stress during neutral landings, initially concentrated on the medial calcaneal surface and inferior tuberosity, intensified with wear, expanding high-stress area by 5.276 cm^2 and increasing peak stress by 22.79 % under EWSC0. For foot inversion, the high-stress region shifted to the inferior tuberosity, with wear reducing peak stress by 10.41 % and eliminating high-stress area in EWSC10 compared to CON10. TSCE analysis revealed that EWSC10 had the lowest stress exposure (0 %kPa) across all conditions. Worn-out shoes would exacerbate heel internal biomechanics, while these effects may be mitigated by foot inversion, likely due to the formation of a relatively flat and larger contact area between the lateral sole and the ground.

1. Introduction

Selecting appropriate footwear for running is crucial, as well-designed shoes can help absorb external forces upon ground impact, potentially reducing the risk of injury (Hamill and Bates, 2023; Lin et al., 2022). However, prolonged use inevitably leads to wear on the shoe sole, primarily manifesting as lateral heel degradation, which is the most common wear pattern (Sole et al., 2014). As this degradation progresses over time, it can lead to increased stiffness and decreased thickness in specific areas, adversely affecting running biomechanics (Kong et al., 2009). Thus, understanding the biomechanical implications of shoe wear is important for safe running.

While previous research has explored the biomechanical effects of shoe degradation, the focus has predominantly been on external factors. For instance, compared to new shoes, worn shoes were found to reduce balance control due to the narrower sole base (S.F. Chen et al., 2023; Chen et al., 2022). During running, the heel plays an important role in managing kinetic energy upon impact, providing essential cushioning for the lower extremities (Li et al., 2022). However, overuse injuries may occur when repetitive loads on heel structure exceed its recovery and remodeling capacity (Mai et al., 2023). Notably, the lateral heel typically contacts the ground first, reflecting foot inversion during the strike phase (Dugan and Bhat, 2005). Degradation in this area may prolong and intensify the inversion, leading to less stable contact and potentially

* Corresponding author.
E-mail address: annie.y.wang@polyu.edu.hk (Y. Wang).

https://doi.org/10.1016/j.jbiomech.2025.112517
Accepted 6 January 2025
Available online 7 January 2025

increasing the risk of overuse injuries (Finestone et al., 2012). Considering that approximately 90 % of recreational runners adopt a rearfoot-strike(RFS) pattern (Larson et al., 2011), it is essential to investigate the internal biomechanical responses of the heel, particularly concerning shoe deterioration and foot inversion, to gain further insights.

In recent decades, finite element(FE) modeling has been increasingly used to study the impact of shoe design on underlying bony structures (Cen et al., 2023; Song et al., 2024, 2023, 2022b). Even-Tzur et al.(2006) initiated the investigation of worn shoes using the FE method and revealed that reduced sole thickness from wear noticeably increased heel pad stress. However, their analysis did not consider shoe degradation patterns or foot inversion, potentially limiting its practical relevance. Meanwhile, most previous foot-shoe FE studies have relied solely on peak stress as a primary metric, which can be misleading as node-based stress calculations do not adequately represent stress distribution across the tissue volume (Fontanella et al., 2013; Yang et al., 2022). Total stress-concentration exposure(TSCE) criteria can serve as a necessary complement as it stands for cumulative amount of stress within the overall region (Katzengold and Gefen, 2019), thereby can offer more details of tissue response characteristics under different shoe wear conditions.

Therefore, the study aim was to explore the influence of simulated shoe degradation and foot inversion on heel plantar pressure and calcaneus stress characteristics at the impact instant during RFS running. We assumed that shoe degradation would result in increased heel pressure and stress concentration in the calcaneus due to reduced sole thickness and uneven sole support. We also hypothesized that foot inversion would further increase the load on the heel, as the altered foot positioning may compromise plantar stability.

2. Methods

2.1. Participant

Given the inherent complexity of the foot-shoe FE model, a single-case design was employed. A participant deemed reasonably representative of recreational runners was selected-a habitual rearfoot strike runner(male, 28 years old, 175 cm in height, and 70 kg in mass) with five years of running experience. The participant reported no musculoskeletal injuries six months before the experiment and provided written consent. This study was conducted in accordance with the Declaration of Helsinki and approved by the ethical committee of the Hong Kong Polytechnic University(HSEARS20240222003).

2.2. Model construction

The model construction details have been reported in our previous studies (Song et al., 2023, 2022a). In brief, we first acquired CT images (1.5 mm slice interval) of the participant's right foot(wearing the shoe) in a neutral position. Then these DICOM data were segmented using Mimic(Materialise, Leuven, Belgium) to extract 3D geometries of the foot bones, soft tissues, and shoe. Finally, these geometries were smoothed using Geomagic Wrap(3D Systems, SC, USA) and imported into SolidWorks(Dassault Systèmes, Paris, France) to construct the coupled model. To retain the basic biomechanical features necessary for addressing the research questions while minimizing model complexity, we included only the posterior half of the model, consisting of the heel bones(calcaneus, talus, distal aspect of the tibia and fibula) and cartilages, soft tissue of the heel, as well as the corresponding upper and sole of the shoe. This approach has been previously employed to strike a balance between model fidelity and computational efficiency (Shaulian et al., 2021).

A widely available running shoe was selected as the reference for the shoe model(heel-to-toe drop: 8 mm). The area of lateral heel degradation was determined using Saito et al.(2007) recommendations as the area between the maximum worn width in the medial–lateral direction (D1 on Fig. 1**A**), maximum worn length in the anterior-posterior direction(D2 on Fig. 1**A**), and maximum worn thickness in the vertical direction(D3 on Fig. 1**B**). Accordingly, three different worn conditions at the heel portion were created in SolidWorks (Fig. 1**C**), 1) New shoe control condition(CON): no wear at the lateral heel portion; 2) Moderate worn shoe condition(MWSC): wear 48.75 mm in width, 52.5 mm in length, and 9 mm in thickness at the lateral heel portion; 3) Excessive worn shoe condition(EWSC): wear 65 mm in width, 70 mm in length, and 12 mm in thickness at the lateral heel portion. Besides, we established heel strike at specific foot inversion angles of 0°, 10°, and 20°, following the settings outlined by Gu et al.(2010) and supported by established biomechanical evidence of heel inversion angles during RFS running (Breine et al., 2017; Mei et al., 2019). In this way, we have 9 foot-shoe combinations in our FE simulation.

All materials assigned to the foot-shoe complex were modeled as homogeneous, isotropic, and linearly elastic (Table 1), which has been shown to provide a reasonable approximation of tissue behavior under running conditions (Zhou et al., 2024). This simplification enabled a more focused analysis of the biomechanical interactions between the heel and shoe without introducing excessive computational complexity, making it particularly effective for evaluating multiple conditions (Zhou et al., 2024). Given the limited data on changes of shoe sole material properties with wear, the Young's modulus of sole was increased by 25 % from the baseline to simulate wear conditions (Even-Tzur et al., 2006). Consisted with previous findings, changes in sole material properties had relatively less influence on heel pressure and calcaneal stress compared to geometrical changes(Supplementary text) (Even-Tzur et al., 2006). A global element size of 3.5 mm was used for the bones, while a 5.0 mm element size for the soft tissue, shoe, and plate(T. L.W. Chen et al., 2023; Wong et al., 2021). Localized mesh refinement was conducted in regions with intricate geometries and the heel impact area. To ensure model accuracy, a mesh convergence analysis was conducted using heel plantar pressure results at running impact. The global mesh size was adjusted by 10 % for each simulation iteration until the deviations in the outcome parameters were reduced to less than 5 % (Henninger et al., 2010). The results of the mesh convergence test indicated changes in pressure values of 1.70 % and 1.89 % compared to the previous and subsequent mesh size modifications, respectively.

2.3. Boundary and loading conditions

The boundary and loading conditions were acquired from the running experiment. The participant was required to complete 3 RFS trials at a speed of 3.33 m/s on a 10-meter runway while wearing the new running shoe. As shown in Fig. 2**A**, foot movements were tracked at 200 Hz using a Vicon motion capture system(Oxford Metrics Ltd., Oxford, UK), while an AMTI force platform(Advance Mechanical Technology Inc., NY, USA) synchronously recorded the ground reaction force (GRF) data at 1000 Hz. The trial that most closely matched the target speed and where the step landed within the force plate was selected for analysis. During the experiment, we also measured the heel plantar pressure data across three shoe conditions using a Pedar insole system (Novel GmbH, Munich, Germany) for model validation.

The running kinematics and kinetics at the impact peak instant(the 1st peak GRF, Fig. 2**B**), including foot strike angle, ankle joint moment, ankle joint reaction force, and vertical GRF, were calculated in OpenSim (SimTK, Stanford, USA) for FE analyses. As shown in Fig. 2**B**, the superior surfaces of the tibia, fibula, and soft tissue as well as the shoe upper tongue, were fully fixed. The angle between the model and plate was then rotated to approximately 15° dorsiflexion in the sagittal plane to simulate the foot position at the heel impact peak instant. Subsequently, the estimated Achilles tendon force(731 N) was applied to the dorsal surface of the calcaneus, and the estimated ankle joint contact force(1185 N) was applied to the superior surface of the talus to represent the landing inertia force. Finally, distinct displacement loads were iteratively applied to the plate towards the model for each

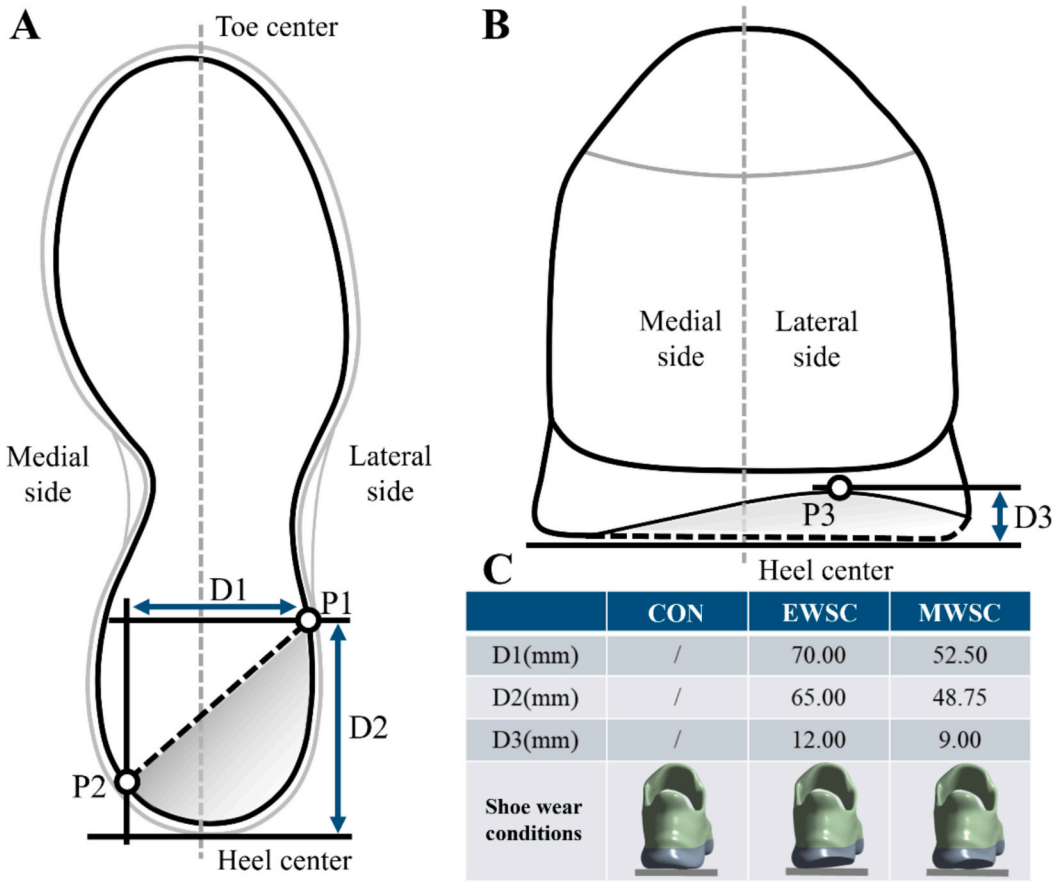

	CON	EWSC	MWSC
D1(mm)	/	70.00	52.50
D2(mm)	/	65.00	48.75
D3(mm)	/	12.00	9.00
Shoe wear conditions			

Fig. 1. Schematic diagram of lateral-heel-worn shoe conditions, A) Bottom view; B) Rear view; C) Hems for measurement of wear. Note: New shoe control condition: CON; Moderate worn shoe condition: MWSC; Excessive worn shoe condition: EWSC; Lateral worn point: P1; Medial worn point: P2; Maximum worn point: P3; Perpendicular distance between P1 and P2: D1; Perpendicular distance between P1 and heel center: D2; Perpendicular distance between P3 and heel center: D3.

Table 1
Element types and material properties for the foot-shoe model components.

Model component	Element type	Young's modulus E (MPa)	Poisson's ratio ν	Mass density ρ (kg/m^3)
Bone	Tetrahedral solid	7300	0.30	1500
Cartilage	Tetrahedral solid	1	0.40	1050
Soft tissue	Tetrahedral solid	1.15	0.49	937
Shoe upper	Tetrahedral solid	11.76	0.35	9400
Shoe sole	Tetrahedral solid	2.739	0.35	2300
Ground plate	Hexahedral solid	17,000	0.10	5000

condition until the simulated force reached the same GRF value obtained from the running trials(1089 N). The coefficient of friction between the foot and shoe, as well as between the shoe and ground plate, was set to 0.6 (Song et al., 2023; Yang et al., 2022).

2.4. Model validation and outcome measures

The foot-shoe FE model has been validated by comparing the predicted pressure with measurements in our previous studies (Song et al., 2023, 2022a). In brief, the Intraclass Correlation Coefficient(ICC) analysis demonstrated excellent concordance between experiments and predictions(ICC score = 0.97; ±95 %CI: 0.93–0.99), and the Bland-Altman plot showed a mean offset of 2.4 kPa, which was not statistically significant($p = 0.71$). In this study, the predicted heel pressure during running across three shoe conditions were compared with the measured data (Fig. 3**A**). The observed 7.2 %–9.1 % peak value difference could be attributed to simplifications in material properties and boundary/loading conditions that were made in the model (Fig. 3**B**). This difference raises some concerns about the external validity of the model, but less than 10 % variability can be considered a fair enough model according to previous reports (Wang et al., 2018; Wong et al., 2015; Malakoutikhah et al., 2022).

For each analysis, we examined the distribution and magnitudes of heel contact pressure and von Mises stress on the calcaneus. The comparison of peak values and the surface area of the top quartile was conducted across the 9 conditions. The TSCE is defined as the area under the stress volumetric exposure curve. We focused on the top quartile of the stress range to evaluate calcaneus exposure to high stress (Katzengold and Gefen, 2019). The volumetric exposure of the calcaneus to von Mises stress was determined by integrating stress values across all calcaneus elements.

3. Results

3.1. Plantar pressure

Distinct trends in pressure distribution and magnitudes were observed as shoes became more worn, depending on the foot inversion angles. In the neutral position(0°), pressure was initially concentrated in the central heel region. As shoe wear increased, the high-pressure area shifted slightly toward the medial heel region and expanded, with its

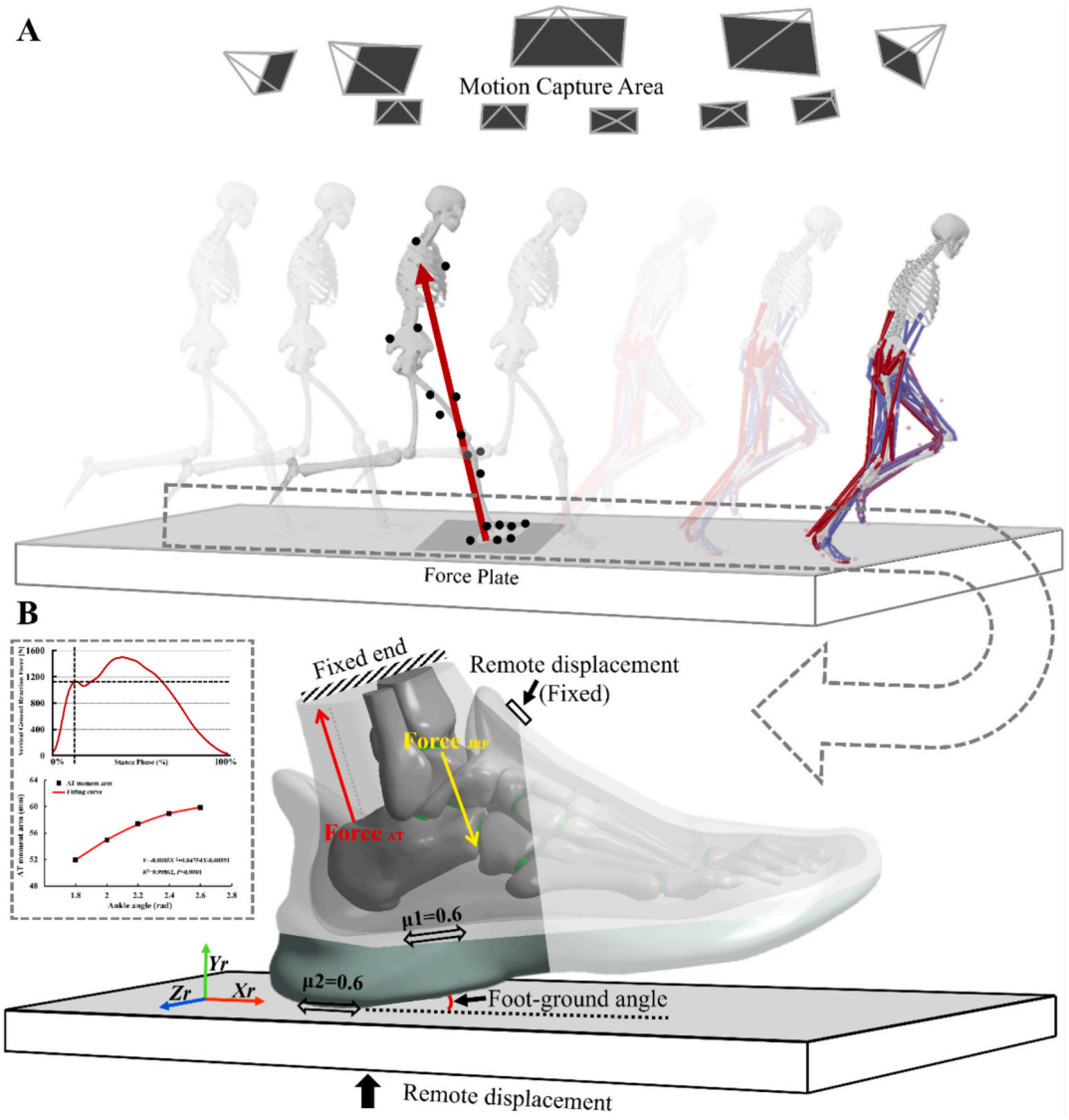

Fig. 2. Subject-specific musculoskeletal simulation of the running gait and boundary/loading conditions for the finite element analyses.

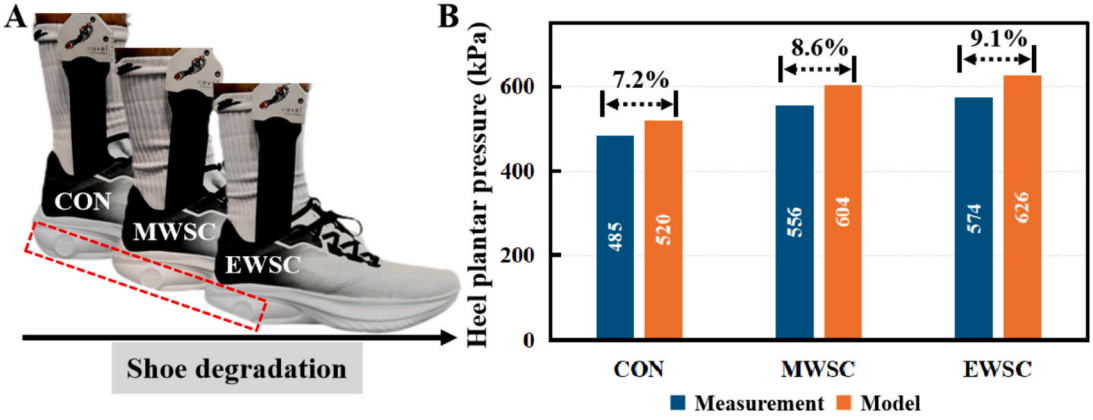

Fig. 3. Comparison of plantar pressure between FE predictions and experimental measurements under different shoe wear conditions for validation. A) lateral-heel-worn shoes used in plantar pressure measurement; B) validation results under different shoe wears conditions.

size increasing by 1 cm^2 in MWSC0 and 1.333 cm^2 in EWSC0 compared to CON0 (Fig. 4**A1**). The peak pressure reached its highest in EWSC0, showing a 24.42 % increase relative to CON0 (Fig. 4**B1**). When landing was simulated with 10° or 20° inversion, the pressure distribution and magnitudes exhibited opposite trends compared to the neutral position. Increased shoe wear resulted in a more even pressure distribution, with

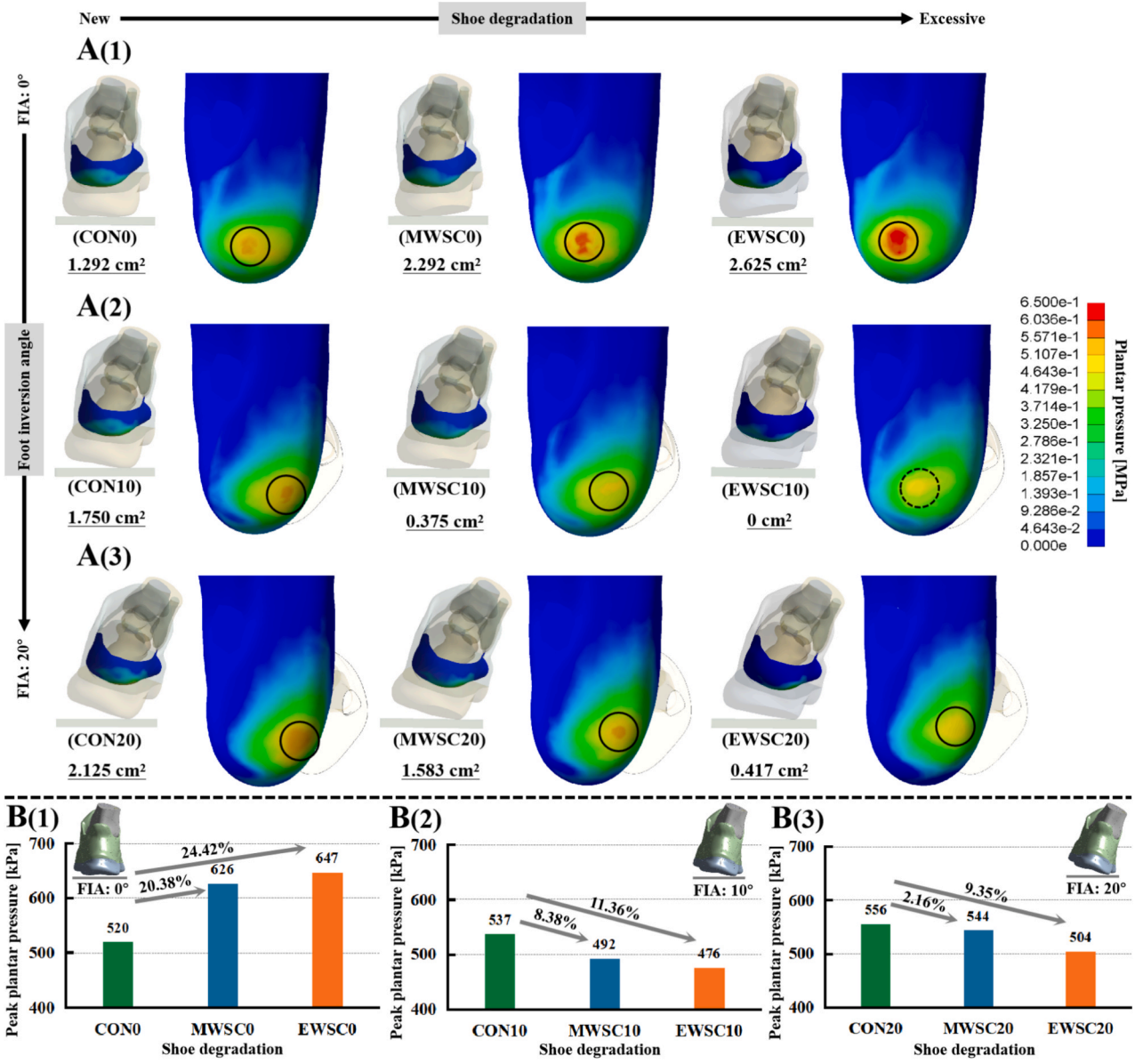

Fig. 4. Comparison of heel plantar pressure in foot-shoe models with respect to different shoe wears and foot inversion angles at the impact peak instant during RFS running. Panel A (1–3) depicts the pressure distribution heatmap of the finite element analysis while panel B (1–3) shows the changes in peak plantar pressure values in respect to the shoe wear conditions in each inversion angle.

the lowest peak pressure recorded in EWSC10, 11.36 % lower than CON10 (Fig. 4**B2**). Under CON10, the pressure shifted to the lateral heel region, whereas under MWSC10 and EWSC10, it gradually redistributed toward the central region with no high-pressure area noted in EWSC10 (Fig. 4**A2**). The MWSC20 and EWSC20 conditions also decreased the heel peak pressure to 2.16 % and 9.35 % less than CON20, respectively (Fig. 4**B3**). Despite the reduction in the high-pressure area in these two conditions relative to CON20, no trend was observed indicating a return of pressure to the central region, as was seen in EWSC10 (Fig. 4**A3**).

3.2. Bone stress

A comparison of bone stress distribution and magnitude also suggested noticeable combined effects of shoe wear and foot inversion. During a neutral foot strike(0°), von Mises stress was concentrated along the medial calcaneal surface and inferior calcaneal tuberosity. Increased shoe wear resulted in larger high-stress areas by 2.772 cm^2 in MWSC0 and 5.376 cm^2 in EWSC0 compared to CON0 (Fig. 5**A1**). Correspondingly, peak stress increased by 9.55 % in MWSC0 and 22.79 % in EWSC0 (Fig. 5**B1**). During 10° and 20° foot inversions, the high-stress region shifted to the inferior calcaneal tubercle, with opposing stress effects observed as shoe wear increased. In MWSC10, increased shoe wear reduced the high-stress area by 0.126 cm^2, and in EWSC10, the high-stress area was absent(0 cm^2) compared to CON10 (Fig. 5**A2**). Meanwhile, peak stress decreased by 3.72 % in MWSC10 and by 10.41 % in EWSC10 (Fig. 5**B2**), with the latter showing the lowest peak stress among all conditions. In MWSC20 and EWSC20, reductions in the high-stress area were also observed, with decreases of 0.378 cm^2 and 0.609 cm^2, respectively, compared to CON20 (Fig. 5**A3**). Peak stress decreased by 10.04 % in MWSC20 and by 14.24 % in EWSC20 (Fig. 5**B3**).

Consistent with the above findings, a comparison of stress exposure on the calcaneus across the models showed a similar trend. Approximately 90 % of the cumulative stress exposure on the calcaneus was concentrated within the 0–1 MPa range (Fig. 6**A1, B1, C1**). Further calculations of TSCE for the highest quartile of the stress range revealed a noticeable increase during neutral foot landings(0°) with shoe wear,

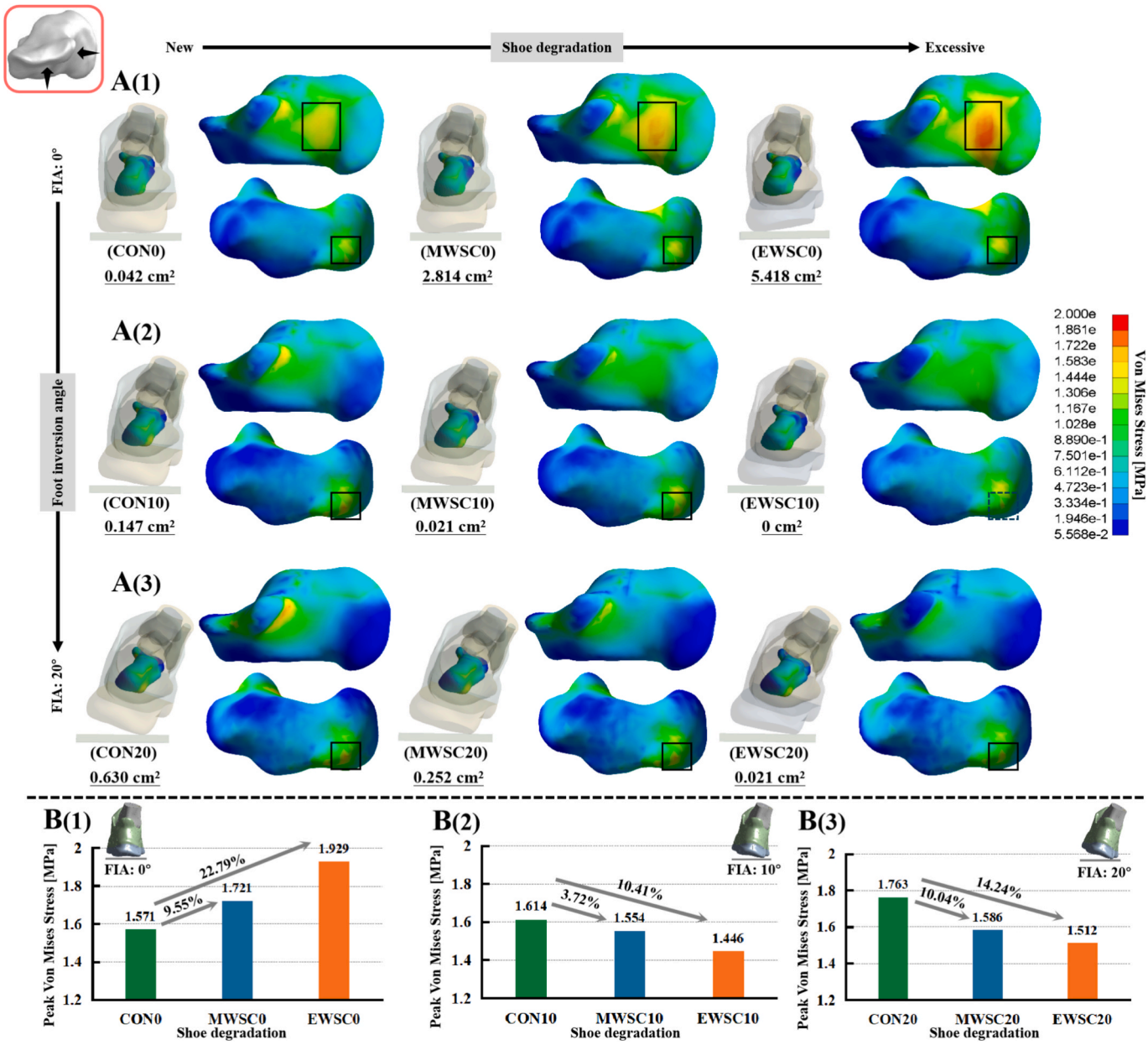

Fig. 5. Comparison of von Mises stress of calcaneal bone in foot-shoe models with respect to different shoe wears and foot inversion angles at the impact peak instant during RFS running. Panel A (1–3) depicts the stress distribution heatmap of the finite element analysis while panel B (1–3) shows the changes in peak von Mises stress values in respect to the shoe wear conditions in each inversion angle.

reaching 76.19 %kPa in MWSC0 and 217.09 %kPa in EWSC0 (Fig. 6**A2**). Conversely, under inversion conditions(10° and 20°), TSCE exhibited a decreasing trend with increased shoe wear. The TSCE decreased to 0.92 %kPa in MWSC10 and to 0 %kPa in EWSC10 compared to CON10 (Fig. 6**B2**), with the latter being the lowest among all conditions. In MWSC20 and EWSC20, the TSCE decreased to 2.48 %kPa and 0.47 % kPa, respectively, compared to CON20 (Fig. 6**C2**).

4. Discussion

While the effect of shoe wear on lower limb biomechanics has been investigated, to the best of our knowledge, this is the first computational simulation to explore the influence of shoe degradation and foot inversion angle on the internal biomechanics of the heel region during RFS running. In this analysis, we assessed the impact of three distinct shoe wear conditions coupled with three different degrees of foot inversion on the distribution and peak value of heel plantar pressure, calcaneus von Mises stress, and the TSCE within the calcaneus bone.

Plantar pressure analysis is a commonly used method to examine foot-shoe interactions during running (Mann et al., 2016). Consistent with our first hypothesis, we observed a noticeable increase in both high-pressure area and peak pressure with the progression of lateral sole wear during neutral position landings. Notably, EWSC0 exhibited the highest values when compared to CON0 (Fig. 4**A1, B1**). This trend aligns with the findings of Even-Tzur et al.,(2006), who reported a 19 % increase in peak heel pad load during running with a 50 % reduction in sole thickness. Their analysis further indicated that changes in material stiffness due to shoe wear had minimal impact on plantar loading, with reduced thickness being the primary factor contributing to increased load. Our study extends these findings by incorporating lateral wear patterns into the analysis of thickness reduction, which offers a more realistic representation of shoe wear (Saito et al., 2007). Lateral wear

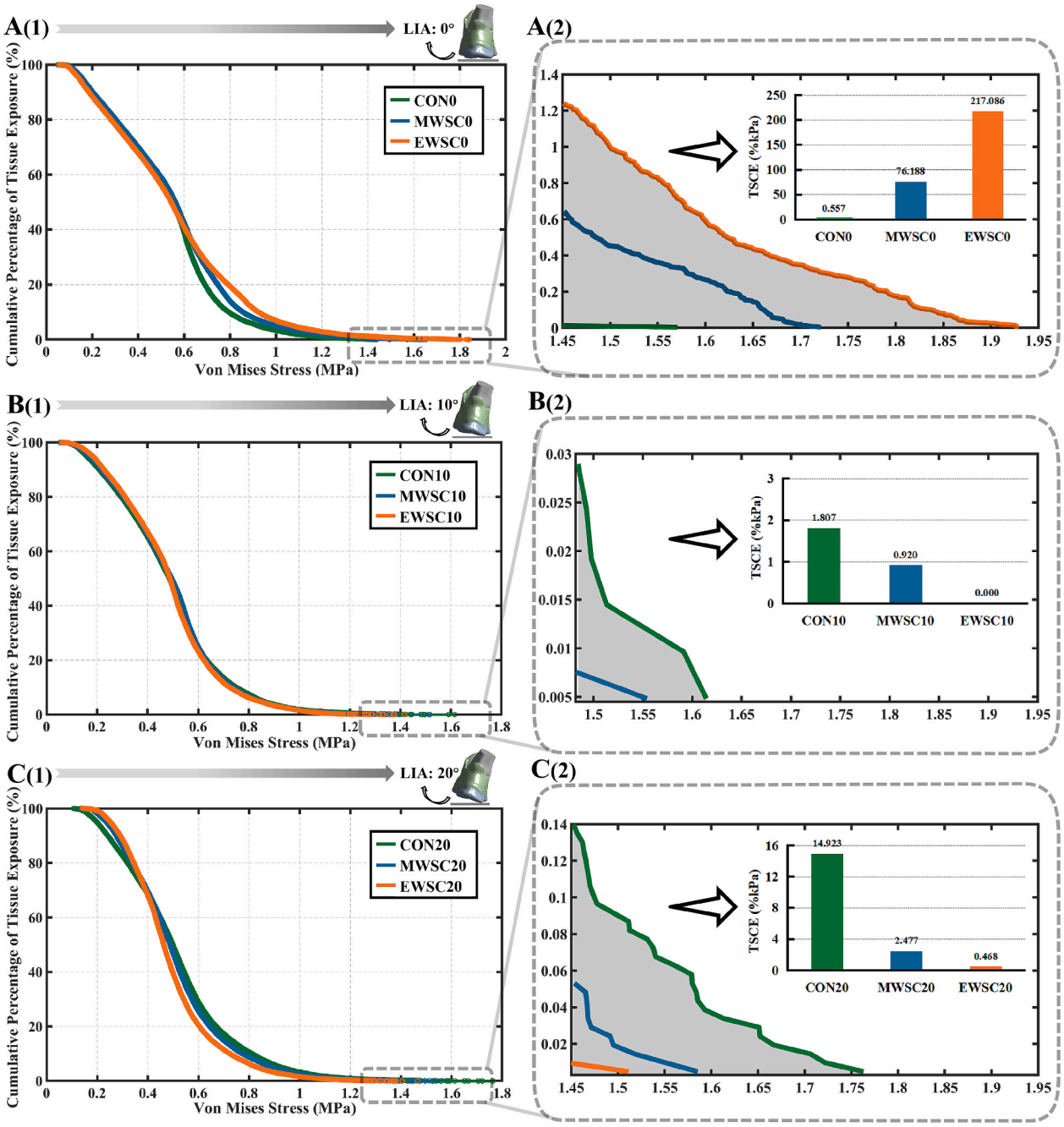

Fig. 6. Comparison of cumulative percentage of calcaneus bone exposure to von Mises stress in respect to the shoe wear conditions in each inversion angle at the impact peak instant during RFS running. Panel A-C (1) depicts the tissue exposure cumulative percentage while panel A-C (2) shows the TSCE for the highest quartile of the calculated stress range.

can compromise the plantar support surface, resulting in reduced sole thickness as well as an asymmetrical and unstable contact base (S.F. Chen et al., 2023; Chen et al., 2022; Saito et al., 2007). Collectively, these factors suggest that the increased peak pressure observed in our study may be attributable to the combined effects of an unstable off-loading surface and reduced sole thickness. This combination likely explains the medial shift of the high-pressure "spot" observed under EWSC0 (Fig. 4**A1**).

Contrary to our second hypothesis, plantar pressure analysis during foot inversion landings showed a different trend. Despite reduced thickness and increased stiffness by shoe wear, lateral heel degradation did not elevate plantar pressure in the heel. Instead, a relatively uniform pressure distribution was observed, particularly under EWSC10, where peak plantar pressure was reduced by 11.36 % and high-pressure areas were absent compared to CON10 (Fig. 4**A2, B2**). The observed pressure reduction effect may seem counter-intuitive, given that inappropriate, worn-out shoes has been postulated as a cause for injuries (Kong et al., 2009; Saito et al., 2007). However, these findings align with previous pressure measurement studies. For example, Rethnam and Makwana (2011) reported that worn running shoes, with an average use of 120.5 weeks, exhibited lower mean peak pressures compared to new shoes. Furthermore, Cornwall and McPoil (2017) analyzed heel-strike runners and found that, after 600 km of use, worn running shoes showed a significant reduction in both the plantar pressure and vertical force at the heel compared to new shoes. From a mechanical perspective, we proposed that the primary mechanism appears to be the formation of a

relatively flat and larger contact area between the lateral sole and the ground due to foot inversion. This pressure reduction is also consistent with the fundamental principle that an increased contact area reduces localized pressure (Bus et al., 2011). Our argument is further supported by the results observed in EWSC20, where the increase in foot inversion angle reduced interface conformity and led to a subsequent rise in plantar pressure (Fig. 4**B3**). It is also noteworthy that the MWSC20 and EWSC20 conditions led to a lateral shift of plantar pressure (Fig. 4**A3**), indicating a displacement of the center of foot pressure(COP) further toward the lateral side. This shift may cause the GRF vector to remain more medial, thereby increasing inversion stress and potentially elevating the risk of lateral ankle sprains under repetitive running loads (Morrison et al., 2010). Thus, runners using worn shoes may need to engage in targeted training to enhance ankle joint stability.

Most injuries sustained during running are overuse injuries, such as stress fractures (van Poppel et al., 2021). Vertical compression has been identified as the primary cause of calcaneal fractures, which highlights the importance of understanding stress characteristics during running strikes (Huang et al., 2024). As illustrated in Fig. 5**A1 and B1**, our study revealed that increased shoe wear during neutral foot landings led to both an expansion in the area and an increase in the amplitude of high stress. The most pronounced increase was observed under EWSC0 on the medial calcaneal surface and the inferior calcaneal tuberosity, which has been previously identified as common fracture sites during running (Vasiliadis, 2017; Vasiliadis et al., 2021). This finding supports existing assertions that shoe wear correlates with a higher incidence of foot stress fractures due to the uneven support provided by worn shoes (Finestone et al., 2012; Frey, 1997). Nevertheless, no prior study has quantitatively examined stress changes in the calcaneus across different heel positions. In our FE analysis, calcaneal stress exhibited a decreasing trend when landing with foot inversion conditions, with the most pronounced reduction observed under EWSC10. Specifically, peak stress decreased by 10.41 % in EWSC10 compared to CON10 (Fig. 5**B2**), and it is also the lowest value among all conditions, which is consistent with the observed reduction in plantar pressure under this condition. The larger contact area between the lateral sole and the ground, as a result of foot inversion, may facilitate a more uniform force transmission, thereby contributing to a decrease in peak stress. Studies on the high-stress area showed a similar trend, with stress concentration shifting towards the inferior calcaneal tubercle, and no high-stress areas were detected under EWSC10 (Fig. 5**A2, A3**). The absence of high-stress areas under EWSC10 may suggest that foot inversions would help redistribute stress at fracture-prone regions when wearing worn shoes, potentially contributing to mitigate the risk of overload stress injuries.

Given that peak stress represents only isolated high-stress instances, we further employed the TSCE criterion to identify volumetric exposures of the calcaneus at high-stress risk, thereby comprehensively evaluate the influence of different shoe wear conditions on heel internal biomechanics (Katzengold and Gefen, 2019). As illustrated in Fig. 6**A2**, TSCE analysis revealed that the EWSC0 condition exhibited the highest volumetric exposure to mechanical stresses in the high-stress domain compared to CON0. Taking into account the findings about peak stress and high-stress areas under this condition, the risk of bone overload may consequently rise due to the accumulation of high stress, especially at the identified fracture sites. On the contrary, minimal volumetric stress exposure was observed under EWSC10 compared to other scenarios (Fig. 6**B2**). This finding further underscores the impact of foot inversions in mitigating excessive stress accumulation under worn shoe conditions. Overall, considering that running strikes often involve a certain degree of foot inversion (Breine et al., 2017; Mei et al., 2019), our findings suggest that avoiding frequent change of running shoes and allowing for sufficient 'wearing-in' of the lateral sole may potentially help mitigate the risk of heel overuse injuries. However, due to the limits of the single-case design, it is not possible to precisely determine the level of wear that would mitigate injury risk. Meanwhile, it is also important to reiterate that the lateral ankle ligaments may experience increased elongation and tension in foot inversion positions, which would result in adverse effects under repetitive running loads. Long-term experimental studies with larger runner cohorts are needed to confirm these matters.

There are limitations in the study. First, our model used a single-case design and did not account for gender variations, which are crucial given the great differences in male and female foot structures and biomechanical responses. Consequently, this design prevents the generalizability of the findings to broader populations. Batch modeling of multiple samples could be a potential solution, yet it might compromise detailed foot geometries and boundary conditions, potentially weakening internal validity (T.L.W. Chen et al., 2023). Second, several simplifying assumptions and approximations were incorporated. For example, some necessary simplifications were made in the structural and material representation of the foot and shoe to constrain the model complexity (Cen et al., 2024; Wang et al., 2015). Meanwhile, although different experimental setups, such as different running surfaces and conditions, may influence simulation input, we kept boundary and loading conditions consistent to create a baseline simulation in which outcome variations could be attributed explicitly to shoe wear and foot inversion effects. Additionally, our model validation did not cover the full variability of real-world running conditions, such as different surfaces. These factors need further exploration to improve the model robustness and applicability. Third, there is no consensus on how shoe sole wear manifests or the exact foot inversion angle during running, as these vary significantly among individuals. Our worn shoe model was based on a generalized definition of shoe degradation (Saito et al., 2007), and foot inversion angles were adapted from commonly reported ranges (Breine et al., 2017; Mei et al., 2019). More importantly, we did not input drastic changes in our shoe model properties due to the lack of reported data on the material property changes of the shoe through the progress of shoe degradation. As such, the interpretation of the obtained results should be undertaken with the consideration of the defined scope and underlying assumptions of the modeling approach. Finally, our study addressed only the acute effects of shoe degradation and foot inversion. Future research should examine their long-term impact on heel biomechanics to provide more guidance for injury prevention and shoe optimization.

5. Conclusions

Increasing lateral sole degradation consistently elevated heel plantar pressure, calcaneus stress, and the TSCE for the high-stress range. Conversely, these effects are mitigated with foot inversions, particularly under EWSC10, which resulted in an 11.36 % reduction in peak pressure, a 10.41 % decrease in peak stress, and no volumetric exposure of the calcaneus to high-stress risk compared to CON10. This reduction likely results from the larger contact area between the lateral sole and the ground due to foot inversion, promoting more uniform force transmission. Accordingly, it is suggested that avoiding frequent change of running shoes and allowing for sufficient 'wearing-in' of the lateral sole may potentially help mitigate the risk of heel overuse injuries. However, runners using worn shoes should engage in targeted training to enhance ankle joint stability. Further research with larger and diverse cohorts is needed to study the long-term effects of worn shoes on heel biomechanics in different running conditions. This will help verify our findings and develop precise recommendations to prevent foot-related issues from improper footwear.

CRediT authorship contribution statement

Yang Song: Writing – original draft, Software, Methodology, Investigation, Conceptualization. **Xuanzhen Cen:** Writing – review & editing, Methodology, Investigation, Conceptualization. **Meizi Wang:** Writing – review & editing, Resources, Investigation, Conceptualization. **Kovács Bálint:** Writing – review & editing, Supervision, Investigation. **Qitao Tan:** Writing – review & editing, Supervision, Formal analysis.

Dong Sun: Writing – review & editing, Validation, Formal analysis. **Shunxiang Gao:** Methodology, Investigation. **Fengping Li:** Methodology, Investigation. **Yaodong Gu:** Writing – review & editing, Supervision, Investigation, Formal analysis. **Yan Wang:** Writing – review & editing, Validation, Supervision, Funding acquisition, Data curation. **Ming Zhang:** Writing – review & editing, Supervision, Investigation, Formal analysis.

Declaration of competing interest

The authors declare that they have no known competing financial interests or personal relationships that could have appeared to influence the work reported in this paper.

Acknowledgment

This study was sponsored by the Research Grants Council (RGC #15211322) and Shenzhen Research Fund (JCYJ-20230807-14041-4029), the authors would like to acknowledge support from the Research Institute for Sports Science and Technology (RISports).

Appendix A. Supplementary data

Supplementary data to this article can be found online at https://doi.org/10.1016/j.jbiomech.2025.112517.

References

Breine, B., Malcolm, P., Van Caekenberghe, I., Fiers, P., Frederick, E.C., De Clercq, D., 2017. Initial foot contact and related kinematics affect impact loading rate in running. J. Sports Sci. 35, 1556–1564.
Bus, S.A., Haspels, R.O.B., Busch-Westbroek, T.E., 2011. Evaluation and optimization of therapeutic footwear for neuropathic diabetic foot patients using in-shoe plantar pressure analysis. Diabetes Care 34, 1595–1600.
Cen, X., Song, Y., Sun, D., Bíró, I., Gu, Y., 2023. Applications of finite element modeling in biomechanical analysis of foot arch deformation: a scoping review. J. Biomech. Eng. 145, 070801.
Cen, X., Song, Y., Yu, P., Sun, D., Simon, J., Bíró, I., Gu, Y., 2024. Effects of plantar fascia stiffness on the internal mechanics of idiopathic pes cavus by finite element analysis: Implications for metatarsalgia. Comput. Methods Biomech. Biomed. Engin. 27, 1961–1969.
Chen, S.F., Wang, Y., Peng, Y., Zhang, M., 2022. Effects of attrition shoes on kinematics and kinetics of lower limb joints during walking. Front. Bioeng. Biotechnol. 10, 824297.
Chen, S.-F., Wang, Y., Peng, Y., Zhang, M., 2023a. Effects of attrition shoes on balance control ability and postural stability following a single-leg drop jump landing. Healthcare. 11, 1127.
Chen, T.-L.-W., Wang, Y., Peng, Y., Zhang, G., Hong, T.-T.-H., Zhang, M., 2023b. Dynamic finite element analyses to compare the influences of customised total talar replacement and total ankle arthroplasty on foot biomechanics during gait. J. Orthop. Transl. 38, 32–43.
Cornwall, M.W., McPoil, T.G., 2017. Can runners perceive changes in heel cushioning as the shoe ages with increased mileage? Int. J. Sports Phys. Ther. 12, 616.
Dugan, S.A., Bhat, K.P., 2005. Biomechanics and analysis of running gait. Phys. Med. Rehabil. Clin. 16, 603–621.
Even-Tzur, N., Weisz, E., Hirsch-Falk, Y., Gefen, A., 2006. Role of EVA viscoelastic properties in the protective performance of a sport shoe: computational studies. Biomed. Mater. Eng. 16, 289–299.
Finestone, A.S., Petrov, K., Agar, G., Honig, A., Tamir, E., Milgrom, C., 2012. Pattern of outsole shoe heel wear in infantry recruits. J. Foot Ankle Res. 5, 1–7.
Fontanella, C.G., Forestiero, A., Carniel, E.L., Natali, A.N., 2013. Analysis of heel pad tissues mechanics at the heel strike in bare and shod conditions. Med. Eng. Phys. 35, 441–447.
Frey, C., 1997. Footwear and stress fractures. Clin. Sports Med. 16, 249–257.
Gu, Y.D., Ren, X.J., Li, J.S., Lake, M.J., Zhang, Q.Y., Zeng, Y.J., 2010. Computer simulation of stress distribution in the metatarsals at different inversion landing angles using the finite element method. Int. Orthop. 34, 669–676.
Hamill, J., Bates, B.T., 2023. Biomechanics and footwear research 1970–2000. Footwear Sci. 15, 123–131.
Henninger, H.B., Reese, S.P., Anderson, A.E., Weiss, J.A., 2010. Validation of computational models in biomechanics. Proc. Inst Mech. Eng. Part H J. Eng. Med. 224, 801–812.
Huang, M., Yu, B., Li, Y., Liao, C., Peng, J., Guo, N., 2024. Biomechanics of calcaneus impacted by talus: a dynamic finite element analysis. Comput. Methods Biomech. Biomed. Engin. 27, 897–904.
Katzengold, R., Gefen, A., 2019. Modelling an adult human head on a donut-shaped gel head support for pressure ulcer prevention. Int. Wound J. 16, 1398–1407.
Kong, P.W., Candelaria, N.G., Smith, D.R., 2009. Running in new and worn shoes: a comparison of three types of cushioning footwear. Br. J. Sports Med. 43, 745–749.
Larson, P., Higgins, E., Kaminski, J., Decker, T., Preble, J., Lyons, D., McIntyre, K., Normile, A., 2011. Foot strike patterns of recreational and sub-elite runners in a long-distance road race. J. Sports Sci. 29, 1665–1673.
Li, J., Song, Y., Xuan, R., Sun, D., Teo, E.-C., Bíró, I., Gu, Y., 2022. Effect of long-distance running on inter-segment foot kinematics and ground reaction forces: a preliminary study. Front. Bioeng. Biotechnol. 10, 833774.
Lin, S., Song, Y., Cen, X., Bálint, K., Fekete, G., Sun, D., 2022. The implications of sports biomechanics studies on the research and development of running shoes: a systematic review. Bioengineering 9, 497.
Mai, P., Robertz, L., Robbin, J., Bill, K., Weir, G., Kurz, M., Trudeau, M., Hollander, K., Hamill, J., Willwacher, S., 2023. Towards functionally individualised designed footwear recommendation for overuse injury prevention: a scoping review. BMC Sports Sci Med Rehabil 15, 152.
Malakoutikhah, H., Madenci, E., Latt, L.D., 2022. The impact of ligament tears on joint contact mechanics in progressive collapsing foot deformity: a finite element study. Clin Biomech. 94, 105630.
Mann, R., Malisoux, L., Urhausen, A., Meijer, K., Theisen, D., 2016. Plantar pressure measurements and running-related injury: a systematic review of methods and possible associations. Gait Posture 47, 1–9.
Mei, Q., Gu, Y., Xiang, L., Baker, J.S., Fernandez, J., 2019. Foot pronation contributes to altered lower extremity loading after long distance running. Front. Physiol. 10, 573.
Morrison, K.E., Hudson, D.J., Davis, I.S., Richards, J.G., Royer, T.D., Dierks, T.A., Kaminski, T.W., 2010. Plantar pressure during running in subjects with chronic ankle instability. Foot Ankle Int. 31, 994–1000.
Rethnam, U., Makwana, N., 2011. Are old running shoes detrimental to your feet? A Pedobarographic Study. BMC Res. Notes 4, 1–5.
Saito, S., Muraki, S., Tochihara, Y., 2007. Effects of worn-out soles on lower limb stability, shock absorption and energy cost during prolonged walking. J. Physiol. Anthropol. 26, 521–526.
Shaulian, H., Gefen, A., Solomonow-Avnon, D., Wolf, A., 2021. Finite element-based method for determining an optimal offloading design for treating and preventing heel ulcers. Comput. Biol. Med. 131, 104261.
Sole, C.C., Milosavljevic, S., Sole, G., Sullivan, S.J., 2014. Patterns of mediolateral asymmetry in worn footwear. Footwear Sci. 6, 177–192.
Song, Y., Cen, X., Zhang, Y., Bíró, I., Ji, Y., Gu, Y., 2022a. Development and validation of a subject-specific coupled model for foot and sports shoe complex: a pilot computational study. Bioengineering 9, 553.
Song, Y., Shao, E., Bíró, I., Baker, J.S., Gu, Y., 2022b. Finite element modelling for footwear design and evaluation: a systematic scoping review. Heliyon 8, e10940.
Song, Y., Cen, X., Chen, H., Sun, D., Munivrana, G., Bálint, K., Bíró, I., Gu, Y., 2023. The influence of running shoe with different carbon-fiber plate designs on internal foot mechanics: A pilot computational analysis. J. Biomech. 153, 111597.
Song, Y., Cen, X., Sun, D., Bálint, K., Wang, Y., Chen, H., Gao, S., Bíró, I., Zhang, M., Gu, Y., 2024. Curved carbon-plated shoe may further reduce forefoot loads compared to flat plate during running. Sci. Rep. 14, 13215.
van Poppel, D., van der Worp, M., Slabbekoorn, A., van den Heuvel, S.S.P., van Middelkoop, M., Koes, B.W., Verhagen, A.P., Scholten-Peeters, G.G.M., 2021. Risk factors for overuse injuries in short- and long-distance running: a systematic review. J. Sport Heal. Sci. 10, 14–28.
Vasiliadis, A.V., 2017. Common stress fractures in runners: an analysis. Saudi J. Sport. Med. 17, 1–6.
Vasiliadis, A.V., Kazas, C., Tsatlidou, M., Vazakidis, P., Metaxiotis, D., 2021. Plantar injuries in runners: is there an association with weekly running volume? Cureus 13, e17537.
Wang, Y., Li, Z., Wong, D.-W.-C., Zhang, M., 2015. Effects of ankle arthrodesis on biomechanical performance of the entire foot. PLoS One 10, e0134340.
Wang, Y., Li, Z., Wong, D.W.C., Cheng, C.K., Zhang, M., 2018. Finite element analysis of biomechanical effects of total ankle arthroplasty on the foot. J. Orthop. Transl. 12, 55–65.
Wong, D.W.C., Wang, Y., Zhang, M., Leung, A.K.L., 2015. Functional restoration and risk of non-union of the first metatarsocuneiform arthrodesis for hallux valgus: a finite element approach. J. Biomech. 48, 3142–3148.
Wong, D.-W.-C., Wang, Y., Niu, W., Zhang, M., 2021. Finite element analysis of subtalar joint arthroereisis on adult-acquired flexible flatfoot deformity using customised sinus tarsi implant. J. Orthop. Transl. 27, 139–145.
Yang, Z., Cui, C., Wan, X., Zheng, Z., Yan, S., Liu, H., Qu, F., Zhang, K., 2022. Design feature combinations effects of running shoe on plantar pressure during heel landing: a finite element analysis with Taguchi optimization approach. Front. Bioeng. Biotechnol. 10, 959842.
Zhou, H., Xu, D., Quan, W., Ugbolue, U.C., Gu, Y., 2024. Effects of different contact angles during forefoot running on the stresses of the foot bones: a finite element simulation study. Front. Bioeng. Biotechnol. 12, 1337540.